Aerosol and Air Quality Research, 10: 540–549, 2010

ISSN: 1680-8584 print / 2071-1409 online
doi: 10.4209/aaqr.2010.05.0036

Correlation between Light Intensity and Ozone Formation for Photochemical Smog in Urban Air of Seoul

Seung-Bok Lee[1,2], Gwi-Nam Bae[1*], Young-Mee Lee[1], Kil-Choo Moon[1], Mansoo Choi[2]

[1] *Global Environment Center, Korea Institute of Science and Technology, 39-1 Hawolgok-dong, Seongbuk-gu, Seoul 136-791, South Korea*
[2] *School of Mechanical and Aerospace Engineering, Seoul National University, Sillim-dong, Gwanak-gu, Seoul 151-744, South Korea*

ABSTRACT

Urban residents are exposed to high levels of ozone that are produced by photochemical reactions of ambient air in strong sunlight. The potential for ozone formation of urban air needs to be characterized in order to avoid exposure to unexpectedly high ozone concentrations during the daytime. In this study, ten sets of twin smog chamber experiments were carried out to determine the correlation between light intensity and ozone formation during photochemical reactions of urban air in Seoul. Single chamber analysis revealed a higher rate of ozone production under higher irradiation than under less intense irradiation under similar initial ambient air conditions. However, the rate of ozone production showed significant variations at the same light intensity. Here, the ratio of two light intensities for both chambers was introduced as a key parameter. The ratio of ozone production was dependent on the ratio of the two light intensities according to a power function with a factor of approximately 1.8. The proposed correlation was used to predict the daytime ozone concentration for calm, clear and dry weather conditions.

Keywords: Ozone production rate; Light intensity; Photooxidation; Twin smog chambers; Urban air.

INTRODUCTION

Photochemical reactions between nitrogen oxides and hydrocarbons in ambient air under solar irradiation, particularly ultraviolet light irradiation, produce ozone in the troposphere. Excessive concentrations of ozone at the ground level are known to have adverse respiratory effects in humans (Seinfeld and Pandis, 1998). In Korea, a high ozone warning system began in 1995 for the protection of public health. The number of days with high ozone episodes, when the hourly-average ozone concentration exceeds 120 ppb, increased from 1 in 1995 to 30 in 2007 (KMOE, 2007, 2008). The annual-average ozone concentration in Seoul, Korea also increased twice from 9 ppb in 1989 to 18 ppb in 2006 (KMOE, 2007). Therefore, predicting the daytime ozone concentration is essential for forecasting the highest ozone concentration of the day in order to avoid exposure to high ozone concentrations.

Many studies have been carried out on complicated numerical simulation models, such as Urban Airshed Model (UAM), Regional Acid Deposition Model (RADM), and Community Multiscale Air Quality (CMAQ) model (Scheffe and Morris, 1993; Dodge, 2000; Appel *et al*., 2007). These numerical simulation models require accurate input data such as precursor emissions and the initial concentrations of chemical compounds. Accumulating a large volume of input data can be expensive. Jeon and Kim (1999) suggested an ozone peak indicator, which is the equivalent of the potential daily maximum ozone concentration that can be estimated by the initial total concentrations of hydrocarbons and nitrogen oxides, with the precursors being the only limiting factor in the development of a simple short-term model for predicting the ozone level. Statistical models used to forecast the ozone concentrations have many limitations. In particular, they do not consider the effect of many factors on the ozone concentration or time delay effects for photochemical reactions (Jeon and Kim, 1999). These approaches need to be performed concurrently to complement their shortcomings for predicting the ozone level more accurately.

The light intensity varies according to the location, season, time of day, and weather conditions. Although urban air has a high potential to form smog, it is less inclined to do so in places where and/or at times when the light intensity is low. Some species, such as NO_2, HCHO,

* Corresponding author. Tel.: 82-2-958-5676;
Fax: 82-2-958-5805
E-mail address: gnbae@kist.re.kr

and HONO, are photolyzed by solar irradiation, particularly ultraviolet light irradiation (Carter *et al*., 1995). The OZIPR (ozone isopleth plotting package for research) includes seventeen photolytic species in the Caltech mechanism (Gery and Corouse, 2002). The rate of NO_2 photolysis (k_1), which is a representative photolytic species, is often used to indicate the light intensity. The value of k_1 for natural sunlight measured at Pasadena, California, USA, at a solar zenith angle of 0° on a clear day is approximately 0.5/min (Cocker III *et al*., 2001).

The indirect effect of the light intensity includes changes in air temperature. The ozone formed in an outdoor smog chamber experiment carried out under high irradiation in spring was approximately six times higher than that carried out under low irradiation in winter, where the cumulative light intensity on a spring day is approximately 2.5 times higher than that on a winter day, and the difference in average temperature is 22°C (Hess *et al*., 1992). A lower temperature is believed to be associated with a lower O_3 concentration due to the increased photochemical lifetime of peroxyacetyl nitrate at a lower temperature, which acts as a sink for both NO_x and radicals (Sillman, 1999).

An experiment on the irradiation of real atmospheric air is called a captive-air irradiation experiment. Many captive-air irradiation experiments have been carried out in outdoor chambers consisting of one to eight reaction bags focusing on the effect of added target species, such as SO_2, liquefied petroleum gas, hydrocarbons, and NO_x (Roberts and Friedlander, 1976; Heisler and Friedlander, 1977; Pitts *et al*., 1977; Kelly, 1987; Kelly and Gunst, 1990; Gunst and Kelly, 1993; Jaimes *et al*., 2003, 2005). Kelly and Gunst (1990) also briefly mentioned the effect of ultraviolet radiation on ozone formation using the 5-day results of other bags filled with a synthetic mixture in outdoor chambers, where the intensity of ultraviolet irradiation could not be controlled.

The photochemical reactions of real ambient air are strongly dependent on the initial urban air quality. Because the ambient air quality changes with time and is not reproducible, two experiments should be carried out simultaneously for examining the effect of single parameter on photochemical reactions in real ambient air. A dual-mode chamber can be used for this purpose. For studies on the effect of light intensity, however, twin smog chambers should be used instead, because the light intensity of each reaction bag can be controlled independently. A comparison of the data from the twin smog chambers with the same initial urban air quality can exclude the effect of the initial urban air quality by using the ratio of variables as discussed later (Kim *et al*., 2009). In this study, twin smog chamber experiments were carried out to determine the correlation between the rate of ozone production and light intensity during the photochemical reactions in real urban air.

In this study, a simple method for predicting the daytime ozone concentration using the experimental correlation between the ozone production rate and light intensity was developed. The effect of temperature change caused by irradiation was not separated from that of the light intensity.

EXPERIMENTAL

Twin smog chambers were installed in a cleanroom at the Korea Institute of Science and Technology (KIST) located in the northeastern Seoul, in which the air temperature and relative humidity were controlled, as shown in Fig. 1 (Bae *et al*., 2003). The two chambers are designated as left and right. Each chamber was illuminated by 64 blacklights (Sylvania, F40/350BL, 40W). Although the overall fluorescent light spectrum emitted from the blacklights is not the same as that of ground-level solar light, the spectrum in the wavelength range of 300–400 nm is close to that of solar light (Cocker III *et al*., 2001; Bae *et al*., 2003). The volume of each cubic-shaped chamber, made from 2-mil (about 51 μm) FEP Teflon film, was approximately 5.8 m^3 (1.8 × 1.8 × 1.8 m) and the surface to volume ratio was 3.3/m.

Urban air was introduced into the chamber through a circular duct using a blower, as shown in Fig. 1. The inlet of the duct was extended to the roof of the building. The duct had two small-branch ducts connected to each chamber. Each small duct had a small fan to inject urban air into the chamber from the main duct. The total length of the sampling ducts for the left and right chambers was approximately 17 m and 19 m, respectively. It took several seconds to transport ambient air from outside to the chambers using a main blower. The loss of gases on the inner surfaces of the sampling ducts was considered negligible due to the short residence time inside the sampling ducts.

Before each experiment, the chambers were flushed continuously with purified air produced by a pure air generator (Aadco Instruments, 737–15) under irradiation for more than 12 hrs and under dark conditions for 2 hrs in order to minimize the effect of chamber contamination. During the flushing process, the background reactivity of the Teflon chambers was examined in a batch mode by irradiating the chambers filled with the purified air for approximately 4 hrs, resulting in an ozone production rate < 0.025 ppb/min. After each experiment, the chambers were flushed again in a similar manner.

After exchanging urban air in the chambers three times for the purpose of conditioning, the urban air was introduced into both chambers for approximately 12 min until the pressure inside chambers reached approximately 1 mmH_2O. After measuring the initial concentrations of the some species in the chambers, they were irradiated with the blacklights in a batch mode for the main experiment. The main experiments started mostly around noon because the above preparation procedures took normally more than 3 hrs.

Four light intensity levels were controlled by changing the number of blacklights switched on (25, 50, 75 and 100% of a total of 64 blacklights). The rate of NO_2 photolysis, which was measured by actinometry experiments using the quartz tube method, ranged from 0.16/min to 0.55/min (Carter *et al*., 1995). The blacklights were replaced once with new ones during the period of the

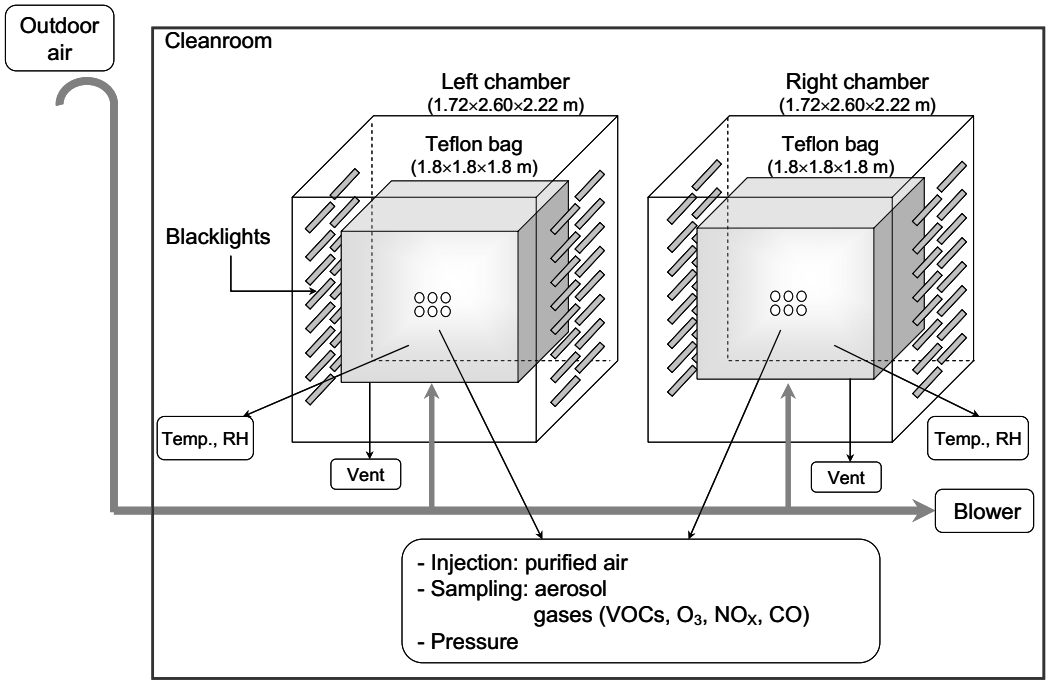

Fig. 1. Schematic diagram of the KIST indoor twin smog chambers.

experiments on 18 February 2004 after use of about two years, which didn't cause much change in UV spectrum measured by an optical spectrum analyzer (Pimacs Co., OSA 300) (Bae *et al*., 2003). Irradiation lasted for approximately 4–5 hrs in each experiment.

During the experiments, the concentrations of O_3, NO-NO_2-NO_x, and CO were monitored every minute using a U.V. photometric O_3 analyzer (TEI, 49C), a chemiluminescence NO-NO_2-NO_x analyzer (TEI, 42C), and a trace level gas filter correlation CO analyzer (TEI, 48C), respectively. The concentrations of benzene, toluene, ethylbenzene, xylene, and toluene-equivalent total volatile organic compounds were analyzed every 25 min by a gas chromatography. The gas chromatography employed an FID detector (Agilent, 6890N) and a 0.32 mm × 30 m × 0.25 μm HP-5 column (Agilent). The sample was concentrated with a preconcentrator (Entech, 7100) to detect low concentrations. The toluene concentration was the second highest among the seventy C_2–C_9 VOCs identified in the urban air of Seoul (Na and Kim, 2001). The air temperature and relative humidity in the chambers were also monitored using a small sensor with a data logger (Sato Keiryoki, SK-L200Th). The sampling lines connected to one set of the measuring equipment were switched from one chamber to the other every 15 min to determine the O_3, NO_x, and CO concentrations, and every 30 min for analysis of the aromatic hydrocarbons. It took approximately 3 min for the gas concentrations to be stabilized after switching sampling lines.

Table 1 gives an outline of the ten experiments carried out from 22 October 2003 to 12 June 2004. Urban air was introduced into the twin chambers in the morning for all experiments, with the exception of the 4L1-2 and 4L2-2 experiments. The difference in the initial CO, O_3, NO_x and toluene concentrations between the twin chambers in most experiments was < 0.02 ppm, 0.9 ppb, 1.3 ppb, and 0.8 ppb, respectively. The NO_2 concentration measured at the national urban air monitoring station was used for the experiments of 2L3-1, 2L4-1 and 4L3-1 because the NO_x analyzer was out of order at that time. Average difference in the NO_2 concentration between the chamber and the urban air monitoring station for other experimental days showing similar ozone concentrations was approximately 20%. The initial toluene concentration ranged from 1.5 to 21.5 ppb with an average of approximately 8.5 ppb, which was slightly higher than the annual average of 6.4 ppb (Na and Kim, 2001).

As listed in Table 1, the air temperature and the relative humidity of outdoor air for experimental days ranged 2–24°C and 26–66%, respectively. After being introduced into the chambers, the temperature was maintained within 21 ± 2°C by an air conditioning system except experiment 2L2-1. For this experiment, the air conditioning system was abnormal. Most of the relative humidity were decreased to < 20% inside the chamber due to the relatively higher temperature than outdoor. This temperature increase might result in a little increase in the ozone production rate, but this effect is the same for twin chambers (Sillman, 1999).

RESULTS AND DISCUSSION

Ozone Production Rate

Fig. 2 shows the changes in the gas concentration in both chambers during the experiment 2L4-2 to demonstrate the time-dependent trends of the gases in the twin smog chambers filled with ambient air. The solid symbols indicate the highly irradiated right chamber and the open symbols denote the lightly irradiated left chamber.

Table 1. Experimental conditions and results of the photochemical reaction of urban air.

Run number[a]	2L2-1	2L3-1	2L4-1	2L4-2	4L1-1	4L1-2	4L2-1	4L2-2	4L3-1	4L3-2
NO_2 photolysis rate[b] (/min)	0.26	0.26	0.26	0.26	0.55	0.55	0.55	0.55	0.49	0.55
	0.27	0.40	0.51	0.51	0.16	0.16	0.31	0.31	0.40	0.45
Experimental date (dd/mm/yy)	12/02/04	22/10/03	24/10/03	13/11/03	23/04/04	28/04/04	09/04/04	16/04/04	30/10/03	12/06/04
Outdoor conditions										
Air temperature (°C)	2[i]	17	12	10	15	19	13[i]	20	13	24
Relative humidity (%)	57[i]	55	51	66	26	40	48[i]	47	48	39
Starting time	12:00	12:19	11:36	11:49	10:47	14:56	11:00	14:30	11:58	12:52
Initial conditions[b]										
Air temperature (°C)	NM[c]	23	22	23	21	20	21	17	23	23
	15	23	NM	23	20	21	20	17	22	22
Relative humidity (%)	NM	24	<20	<20	<20	<20	<20	40	<20	33
	<20	31	NM	<20	<20	<20	<20	40	<20	39
O_3 (ppb)	1.5	24.7	1.7	4.5	27.0	36.7	14.5[f]	48.7	1.5	50.7
	1.6	23.8	1.8	5.4	27.2	38.0	15.1[f]	50.3	1.7	49.9
NO (ppb)	32.3	0[h]	21[h]	BDL[d]	0.4	0.9	1.4	1.0	20.5[h]	0.6
	31.3	0[h]	21[h]	BDL	0.5	0.8	0.8	0.9	20.5[h]	0.4
NO_2 (ppb)	62.5	16[g]	42[g]	34.3	15.2	37.2	49.6	22.6	41[g]	5.5
	61.3	16[g]	42[g]	34.0	15.5	38.6	50.0	23.7	41[g]	5.8
CO (ppm)	0.579	0.380	0.695	0.456	0.618	0.879	0.904	0.974	0.681	BDL
	0.559	0.352	0.706	0.451	0.613	0.884	0.885	0.977	0.671	BDL
Toluene (ppb)	5.6	17.6	11.0	4.4	2.5	8.7	5.9	6.1	14.9	1.5
	5.2	21.5	11.5	3.6	2.4	7.5	5.8	5.7	15.6	2.1
TVOC[e] (ppb)	36.1	47.7	66.2	27.1	15.9	37.6	35.9	36.8	69.7	2.9
	33.3	50.4	67.6	23.0	15.6	36.5	33.9	34.8	66.1	4.9
TVOC/NO_x (ppbC/ppb)	2.7	20.9	7.4	5.5	7.1	6.9	4.9	10.9	7.9	3.2
	2.5	22.1	7.5	4.6	6.8	6.5	4.7	9.9	7.5	5.5
Irradiation time (min)	296	272	245	275	260	262	247	248	328	255
Experimental results[b]										
O_3 production rate (ppb/min)	0.02	0.20	0.03	0.05	0.10	0.23	0.10	0.35	0.15	0.18
	0.02	0.39	0.10	0.15	0.01	0.03	0.05	0.11	0.09	0.13
Constant C	0.26	2.30	0.33	0.56	0.28	0.67	0.29	1.02	0.53	0.52
	0.26	2.00	0.34	0.50	0.24	0.77	0.37	0.91	0.49	0.54

[a] aLb-c: a and b indicate the level of light intensity for the left chamber and the right chamber, respectively, and c is frequency of the experiment.
[b] First row: left chamber, second row: right chamber
[c] Not measured.
[d] Below lower detection limit.
[e] Toluene-equivalent concentration of total VOCs measured with GC-FID.
[f] Ozone was injected using an ozone generator.
[g] 1-h average data measured at the Gileum-dong ambient air pollution monitoring station, Seoul, Korea.
[h] For the 2L2-1 experiment with initial conditions similar to the 2L3-1, 2L4-1, and 4L3-1 experiments, the initial O_3 concentrations were < 2 ppb and the concentration ratios of NO/NO_2 were approximately 0.5. Therefore, the NO concentration was assumed to be the half of the NO_2 concentration because the initial O_3 concentration was below 2 ppb.
[i] Daily average data obtained from surface synoptic station of Seoul because of no measured data.

Under dark conditions prior to irradiation, the NO_2 concentration increased due to a reaction between O_3 and NO. After the blacklights were turned on (irradiation time = 0 min), NO_2 photolysis occurred within a short period of time, resulting in a rapid increase in the NO and O_3 concentrations. Thereafter, the O_3 concentration in the chamber increased almost linearly. The rate of ozone production was obtained from a linear regression curve based on this linearly increasing period from 20-min irradiation to 240-min irradiation. The rate of ozone production increased three times higher in the high intensity chamber.

In order to compare photooxidation stages between fresh and aged ambient air, the typical time-series plot of gas concentrations for a synthetic toluene-NO_x-purified air mixture from Lee *et al*. (2005) is shown in Fig. 3. This

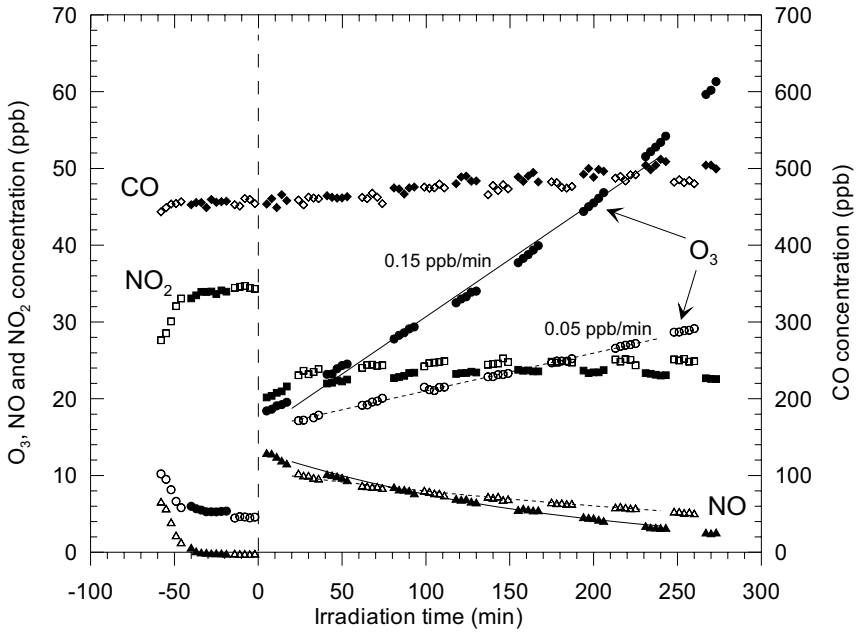

Fig. 2. Changes in the gas concentrations for the 2L4-2 experiment. The open and solid symbols represent the data for the left chamber with $k_1 = 0.26$/min and the right chamber with $k_1 = 0.51$/min, respectively.

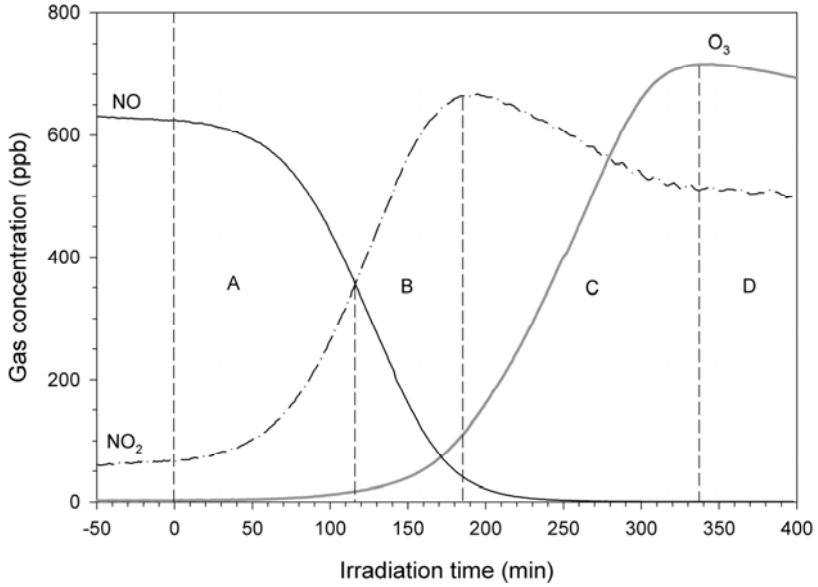

Fig. 3. Typical change in the gas concentrations during the photochemical reactions of a synthetic toluene-NO_x-air mixture with a higher concentration. The data is from the A06R06 experiment reported by Lee *et al.* (2005), whose initial toluene and NO_x concentrations and their ratio were 557 ppb, 691 ppb, and 5.6 ppbC/ppb, respectively.

experiment conducted in the same chamber facility was chosen for more clear comparison and consistency, although the similar pattern of gases is also found in other chamber experiment with relatively low precursor concentrations (Simonaitis *et al*., 1997). Even though the initial toluene and NO_x concentrations were 557 ppb and 691 ppb, respectively, which are much higher than those of ambient air in this study, it can give an insight on fresh ambient air that contains precursors recently emitted into atmosphere.

As shown in Fig. 3, in general, an induction time (period A) is needed to form significant amounts of ozone after irradiation, and the ozone concentration can reach its maximum after further irradiation for a toluene-NOx–air mixture experiment, and then it decreases slowly after the maximum. The ozone concentration curve looks like an S-shape. As shown in Fig. 2, however, the ozone concentration curve of real urban air shows an L-shape after irradiation. Here, the sharp jump of ozone concentration occurred just after irradiation adjacent to vertical dotted line representing starting time and the nearly linear curve of ozone concentration during the irradiation form the L-shape. This was attributed to the ambient air undergoing a

slight photooxidation process outside before entering the chambers.

In Fig. 2, the NO_2 concentration reached its maximum during the course of the experiment 2L4-2 and the change in O_3 concentration with irradiation time appears linear. Therefore, the entire reaction period of ambient air for 2L4-2 is believed to correspond to the transit from period B to period C observed in the synthetic mixture experiment, as shown in Fig. 3.

All experiments may correspond to periods B or C because the NO_2 concentration was higher than the NO concentration and the O_3 concentration did not reach its maximum in any of the experiments. The change in the gas profiles for the four experiments (2L2-1, 2L4-1, 2L4-2, 4L3-1) and others (2L3-1, 4L1-1, 4L1-2, 4L2-1, 4L2-2, 4L3-2) is similar to that of periods B and C, respectively. The initial O_3 and NO_x concentrations of the former were relatively low and high, respectively, compared to the latter. It implies that the photooxidation stages of ambient air can be determined according to the initial ambient air quality. As shown in Fig. 4, although the photooxidation stages of ambient air in the experiments of 4L2-1 and 4L2-2 were similar and the light intensities were the same, there was a significant difference in the rate of ozone production. This is due to the difference in ambient air day by day. For example, the rate of ozone production varied from 0.023 ppb/min to 0.21 ppb/min at a k_1 of approximately 0.3/min, and ranged from 0.094 ppb/min to 0.34 ppb/min at a k_1 of approximately 0.5/min. Therefore, it is difficult to find a correlation between the rate of ozone production and light intensity for photochemical reactions of urban air from single chamber data.

In order to examine the photooxidation process, NO was chosen instead of toluene because both the initial toluene concentration and amount of reacted toluene were low, and its measurement interval was large. As shown in Fig. 2, the rate of NO loss due to photochemical reactions in the chamber with higher levels of irradiation was greater than that in the chamber with lower levels of irradiation. The rate of NO loss was calculated using an exponential decay curve fit. The change in the NO concentration can be expressed as an exponential function if k is assumed to be the average reaction rate for all oxidants and the total concentration of oxidants reacting with NO is assumed to be almost constant during the experiment, as shown in Eq. (3).

$$NO + oxidants \rightarrow NO_2 \tag{1}$$

$$\frac{d[NO]}{dt} = -k[NO] \times [oxidants] \tag{2}$$

$$[NO] = [NO]_0 \exp(-k[oxidants] \times t) \tag{3}$$

The coefficients of the exponential function fit for the NO concentration measured from 20-min to 240-min irradiation were calculated for twin chambers. Fig. 5 shows the ratio of k_1 in the left chamber to that in the right chamber. Here, three experiments (2L3-1, 2L4-1, 4L3-1) were excluded due to missing data and one experiment (4L3-2) was not considered because of the low NO concentration, < 1.5 ppb.

As shown in Fig. 5, the NO decay rate was proportional to k_1, which suggests that the amount of oxidants reacting with NO increased linearly with k_1. If there are no oxidants except for ozone, ozone cannot accumulate, and the NO and NO_2 concentrations would not change due to the reactions expressed in Eqs. (1), (4) and (5).

$$NO_2 \xrightarrow{h\nu} NO + O \tag{4}$$

$$O_2 + O \rightarrow O_3 \tag{5}$$

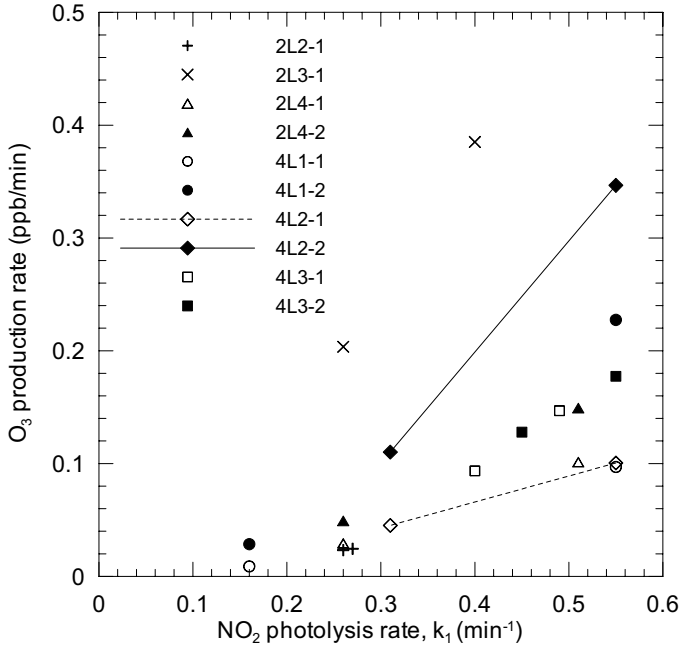

Fig. 4. Dependency of the ozone production rate for the photochemical reactions of urban air on the NO_2 photolysis rate.

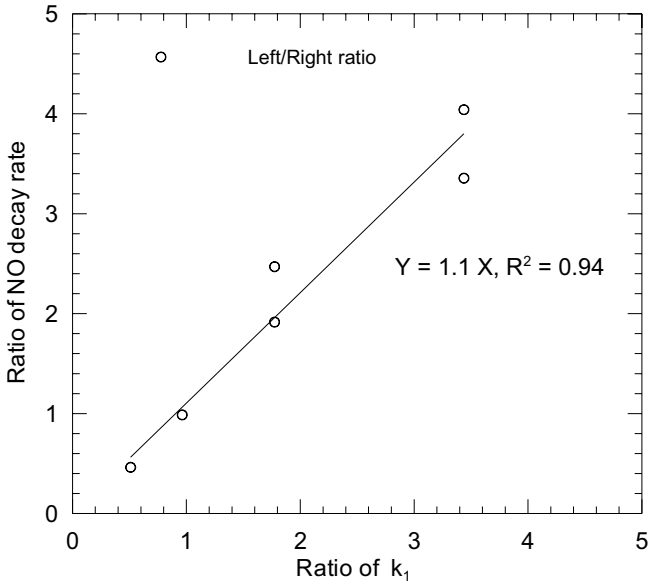

Fig. 5. Effect of light intensity on the NO decay rate for the photochemical reactions of urban air obtained by twin chamber analysis.

If the amount of oxidants except for ozone in ambient air is assumed to increase approximately by a factor of x when k_1 increases by a factor of x, the conversion rate from NO to NO_2 would increase by a factor of x. Finally, the ozone production rate would increase by a factor of x^2 by virtue of simultaneous increase in both the conversion rate from NO to NO_2 and the NO_2 photolysis rate, k_1. However, the factor of x^2 must be changed slightly because there are other reactions, such as a reaction between NO_2 and radicals to form HNO_3 or peroxyacetyl nitrate.

The CO concentration in the chamber with a higher ozone concentration was 1–4% higher than that in the chamber with a lower ozone concentration, since it is a product (Stockwell *et al*., 1997).

Experimental Correlation between Ozone Production Rate and Light Intensity

In this study, the data from the twin chambers with the same initial urban air quality were compared in order to exclude the effect of the initial urban air quality. Fig. 6 shows the ratio of the ozone production rates between the two chambers as a function of the ratio of k_1 of the left chamber to that of the right. The correlation between the ratio of k_1 and the ratio of the ozone production rates could be represented as a power function curve passing through a point (1, 1) with a power of approximately 1.8. Therefore, the rate of ozone production can be expressed as a power function as per Eq. (6), and the results of the above twin chambers analysis can be written as Eq. (7).

$$O_3 \ production\ rate = Ck_1^{1.8} \tag{6}$$

$$\frac{O_3 \ prodcution\ rate_{left}}{O_3 \ prodcution\ rate_{right}} = \frac{Ck_{1,left}^{1.8}}{Ck_{1,right}^{1.8}} = \left(\frac{k_{1,left}}{k_{1,right}}\right)^{1.8} \tag{7}$$

where C is a constant which can be regarded as the ozone formation potential on photochemical reactivity, which can be determined for given urban air samples. In this study, the value of C ranged from 0.2 to 2.3. Since the ozone formation potential can be affected by factors such as the initial precursor concentration, it is likely that the value of C is a function of those factors. Although the correlation between C and the initial precursor concentration is difficult to determine due to the lack of measured species and the relatively low number of experiments in this study, experiments with a higher C value ranging from 0.9 to 2.3 had a $TVOC/NO_x$ ratio > 9. The correlation between the light intensity and rate of ozone production can be used to estimate the daytime O_3 concentration using the O_3 concentration in the morning of the same day.

In this study, the effect of temperature was not separated from that of the light intensity. The light intensity was controlled by adjusting the number of illuminated blacklights. Hence, the air temperature in the chamber changed due to the heat emitted from the blacklights. In the case of the ozone formation shown in Fig. 4, the maximum temperature difference between the twin chambers during irradiation was 13°C for the experiment 4L1-2, where the ratio of k_1 was 3.4. In this case, the ratio of the ozone production rates was 8. This is comparable to outdoor smog chamber results, in which there was maximum temperature difference of approximately 22°C between the experiments on a spring and winter day, and the ratios of the cumulative light intensities and consequent ozone concentrations measured in the afternoon were approximately 2.5 and 6, respectively (Hess *et al*., 1992).

Prediction of Daytime Ozone Concentration

In order to predict the daytime O_3 concentration using a proposed correlation, the ozone production rate in the morning and k_1 value at that time are required. To illustrate

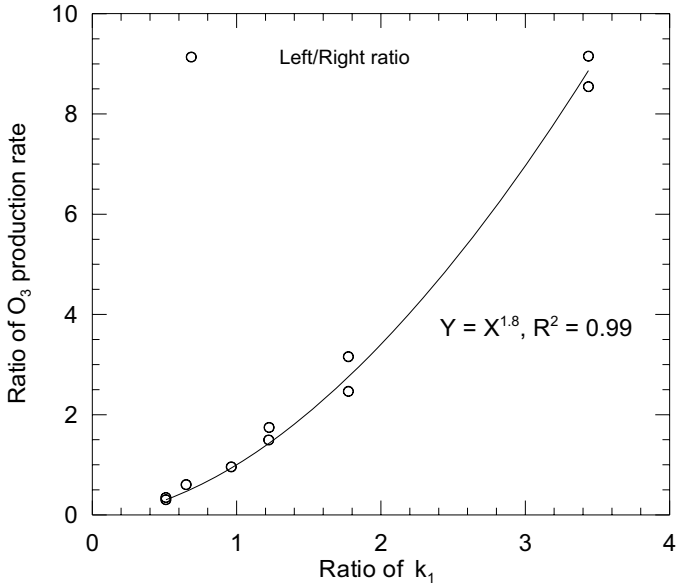

Fig. 6. Effect of light intensity on the rate of ozone production for photochemical reactions of urban air obtained by twin chamber analysis.

the applicability of the proposed correlation, Fig. 7(a) shows the O_3 concentration measured on a clear day, 9 April 2004 at the Gileum-dong ambient air monitoring station, which is the nearest station to the KIST, and is managed by the Ministry of Environment, Korea. On that day, the daily averages of air temperature, relative humidity and wind speed were 13°C, 48% and 2.7 m/s, respectively, which were similar to the monthly averages of April 2004. The ozone production rate in the morning, $(O_3 \text{ production rate})_{t8\text{-}9}$ in Eq. (8) was calculated to be 0.08 ppb/min from the two hourly-average concentrations at 8:00 a.m. and 9:00 a.m. The value was corrected to 0.10 ppb/min considering the dilution effect due to increment of mixing layer height. The data of the mixing layer height of the troposphere in Seoul were reported by Park *et al*. (2002). The k_1 from 8:00 a.m. to 9:00 a.m. ($k_{1,t8\text{-}9}$ in Eq. (8)) was assumed to be constant, 0.29/min. The k_1 values with time on that day in Fig. 7(a) were obtained from the OZIPR model (Gery and Corouse, 2002). The O_3 concentration at time j can be used to predict the O_3 concentration at time i with the ozone production rate (ppb/min) multiplied by 60 min according to the following Eq. (8).

$$[O_3]_{t_j} = [O_3]_{t_i} + (O_3 \ production\ rate)_{t_{8-9}} \left(\frac{k_{1,t_{i-j}}}{k_{1,t_{8-9}}} \right)^{1.8} \times 60 \qquad (8)$$

The predicted O_3 concentrations with time were significantly higher than the monitored data shown in Fig. 7(a) because the increment of mixing layer height was not considered at this step. The re-predicted O_3 concentrations considering the increment of mixing layer height were similar to the monitored data.

Another prediction example of O_3 concentration on 16 April 2004 obtained through the same process is shown in Fig. 7(b). On that day, the daily averages of air temperature, relative humidity and wind speed were 16°C, 52% and 3.7 m/s, respectively, which were relatively favorable to mixing and dilution compared to the monthly averages of April 2004. This meteorological condition could be one of the reasons why actual O_3 concentrations are a little lower than the predicted values as shown in Fig. 7(b).

This paper demonstrates a simple method for predicting the daytime O_3 concentration using the ozone production rate measured in the morning of that day. The assumptions used to develop this simple method were: first, both emissions of precursors in urban areas and the transport of air mass from the other area were not significant during the daytime; second, a mixing layer height might not change greatly during the daytime, compared with the typical data of the season; third, the meteorological conditions between morning and daytime were unchanged except for the light intensity.

The daytime O_3 concentrations were predicted using the rate of ozone production measured in the morning by virtue of the experimental correlation between the rate of ozone production and light intensity from the experimental method developed using the twin smog chambers.

This method can assist in understanding the role of light intensity on photooxidation reactions in ambient air without the need to process a large volume of data.

CONCLUSIONS

The relationship between light intensity and ozone formation for photochemical smog in real urban air was examined using indoor twin smog chambers. In each experiment, the rate of ozone production increased with increasing light intensity. No induction time was ahead of ozone formation for ambient air introduced into the smog chambers in the morning.

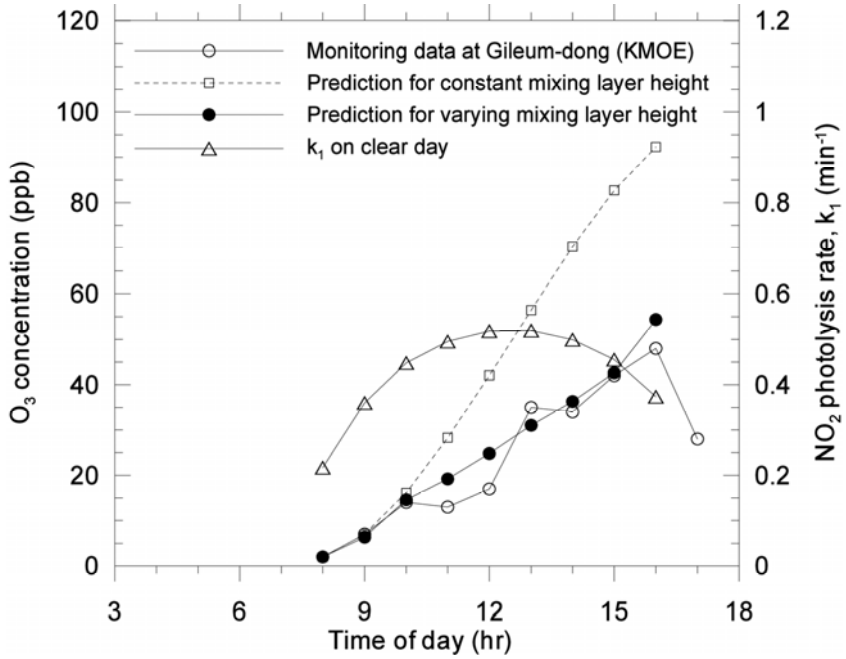

(a) 9 April 2004

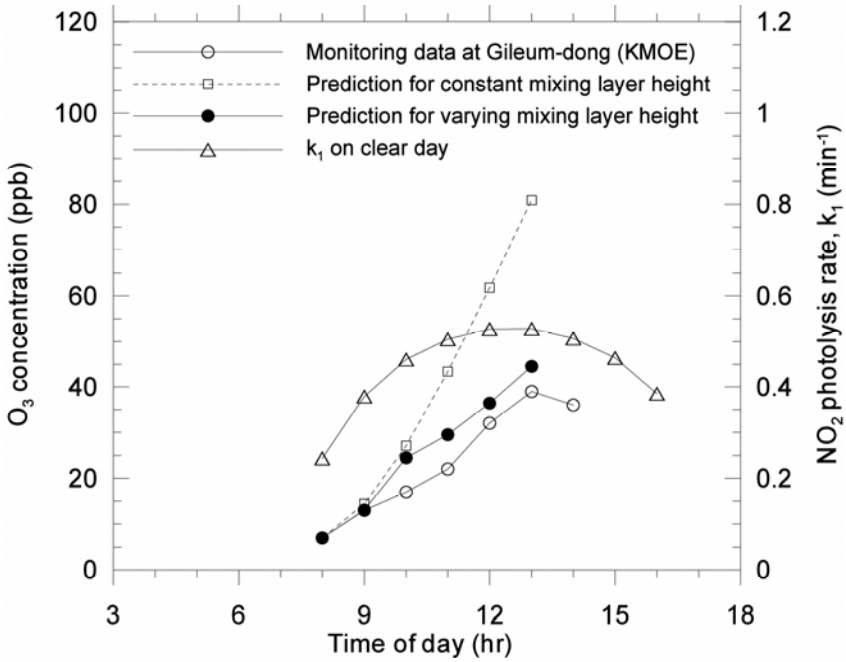

(b) 16 April 2004

Fig. 7. Prediction of the daytime O_3 concentration using a proposed correlation between the light intensity and ozone production rate.

Excluding the effect of the initial urban air quality, the ratio of the ozone production rates increased with increasing ratio of NO_2 photolysis rates, k_1, according to a power function of power 1.8. This correlation suggests that the rate of ozone production was proportional to $k_1^{1.8}$. The fact that the NO decay rate was linearly proportional to k_1 supports this explanation.

In conclusion, the daytime O_3 concentration could be estimated using the rate of ozone production determined in the morning of a clear day. The proposed correlation between ozone production rate and light intensity is limited to calm, clear and dry days. Further studies are needed to account for windy, cloudy, and humid weather conditions.

ACKNOWLEDGMENTS

This study was supported by the National Research Laboratory Program of the Korean Ministry of Science and Technology (contract No. M1-0204-00-0049) and by the Korea Institute of Science and Technology.

REFERENCES

Appel, K.W., Gilliland, A.B., Sarwar, G., and Gilliam, R.C. (2007). Evaluation of the Community Multiscale Air Quality (CMAQ) Model Version 4.5: Sensitivities Impacting Model Performance Part I- Ozone. *Atmos. Environ.* 41: 9603–9615.

Bae, G.N., Kim, M.C., Lee, S.B., Song, K.B., Jin, H.C., and Moon, K.C. (2003). Design and Performance Evaluation of the KIST Indoor Smog Chamber (in Korean). *J. Korean Soc. Atmos. Environ.* 19: 437–449.

Carter, W.P.L., Luo, D., Malkina, I.L., and Pierce, J.A. (1995). *Environmental Chamber Studies of Atmospheric Reactivities of Volatile Organic Compounds - Effects of Varying Chamber and Light Sources.* Final Report to National Renewable Energy Laboratory, Contract XZ-2-12075, Coordinating Research Council, Inc., Project M-9, California Air Resources Board, Contract A032-0692, South Coast Air Quality Management District, Contract C91323, University of California, Riverside.

Cocker III, D.R., Flagan, R.C., and Seinfeld, J.H. (2001). State-of-art Chamber Facility for Studying Atmospheric Aerosol Chemistry. *Environ. Sci. Technol.* 35: 2594–2601.

Dodge, M.C. (2000). Chemical Oxidant Mechanisms for Air Quality Modeling: Critical Review. *Atmos. Environ.* 34: 2103–2130.

Gery, M.W. and Corouse, R.R. (2002). User's Guide for Executing OZIPR. US EPA Home Page (http://www.epa.gov/scram001/models/other/oziprdme.txt).

Gunst, R.F. and Kelly, N.A. (1993). Captive-air Irradiation Experiments on Ozone Formation in Southern California. *Technometrics* 35: 256–267.

Heisler, S.L. and Friedlander, S.K. (1977). Gas-to-particle Conversion in Photochemical Smog: Aerosol Growth Laws and Mechanisms for Organics. *Atmos. Environ.* 11: 157–168.

Hess, G.D., Carnovale, F., Cope, M.E., and Graham, M.J. (1992). The Evaluation of Some Photochemical Smog Reaction Mechanisms - I. Temperature and Initial Composition Effects. *Atmos. Environ.* 26: 625–641.

Jaimes, J.L.L., Sandoval, J.F., González, U.M., and González, E.O. (2003). Liquefied Petroleum Gas Effect on Ozone Formation in Mexico City. *Atmos. Environ.* 37: 2327–2335.

Jaimes, J.L.L., Sandoval, J.F., González, E.O., Vázquez, M.G., González, U.M., and Zambrano, A.G. (2005). Effect of Liquefied Petroleum Gas on Ozone Formation in Guadalajara and Mexico City. *J. Air Waste Manage.* 55: 841–846.

Jeon, E.C. and Kim, J.W. (1999). Development of a Short-term Model for Ozone using OPI (in Korean). *J. Korean Soc. Atmos. Environ.* 15: 545–554.

Kelly, N.A. (1987). The Photochemical Formation and Fate of Nitric Acid in the Metropolitan Detroit Area: Ambient, Captive-air Irradiation and Modeling Results. *Atmos. Environ.* 21: 2163–2177.

Kelly, N.A. and Gunst, R.F. (1990). Response of Ozone to Changes in Hydrocarbon and Nitrogen Oxide Concentrations in Outdoor Smog Chambers Filled with Los Angeles Air. *Atmos. Environ.* 24: 2991–3005.

Kim, Y.J., Platt, U., Gu, M.B., and Iwahashi, H. (2009). *Atmospheric and Biological Environmental Monitoring*, Springer.

KMOE (Korea Ministry of Environment) (2007). *Annual Report of Air Quality in Korea 2006.* Report No. 11-1480000-000532-10, National Institute of Environmental Research.

KMOE (Korea Minstry of Environment) (2008). *Status of Ozone Warning Episode in the Year of 2007.* Available from http://www.me.go.kr/, accessed on March 13, 2008.

Lee, Y.M., Bae, G.N., Lee, S.B., Kim, M.C., and Moon, K.C. (2005). Effect of Initial Toluene Concentration on the Photooxidatioin of Toluene-NO_x-air Mixture - I. Change of Gaseous Species (in Korean). *J. Korean Soc. Atmos. Environ.* 21: 15–26.

Na, K. and Kim, Y.P. (2001). Seasonal Characteristics of Ambient Volatile Organic Compounds in Seoul, Korea. *Atmos. Environ.* 35: 2603–2614.

Park, S.S., Kim, Y.J., and Fung, K. (2002). $PM_{2.5}$ Carbon Measurements in Two Urban Areas: Seoul and Kwangju, Korea. *Atmos. Environ.* 36: 1287–1297.

Pitts Jr, J.N., Smith, J.P., Fitz, D.R., and Grosjean, D. (1977). Enhancement of Photochemical Smog by *N,N'*-Diethylhydroxylamine in Polluted Ambient Air. *Science* 197: 255–257.

Roberts, P.T. and Friedlander, S.K. (1976). Photochemical Aerosol Formation SO_2, 1-Heptene, and NO_x in Ambient Air. *Environ. Sci. Technol.* 10: 573–580.

Scheffe, R.D. and Morris, R.E. (1993). A Review of the Development and Applications of the Urban Airshed Model. *Atmos. Environ.* 27: 23–39.

Seinfeld, J.H. and Pandis, S.N. (1998). *Atmospheric Chemistry and Physics,* John Wiley & Sons, New York.

Sillman, S. (1999). The Relation between Ozone, NO_x and Hydrocarbons in Urban and Polluted Rural Environments. *Atmos. Environ.* 33: 1821–1845.

Simonaitis, R., Meagher, J.F., and Bailey, E.M. (1997). Evaluation of the Condensed Carbon Bond (CB-IV) Mechanism Against Smog Chamber Data at Low VOC and NO_x Concentrations. *Atmos. Environ.* 31: 27–43.

Stockwell, W.R., Kirchner, F., Kuhn, M., and Seefeld, S. (1997). A New Mechanism for Regional Atmospheric Chemistry Modeling. *J. Geophys. Res.* 102: 25847–25879.

Received for review, May 1, 2010
Accepted, August 23, 2010